applied sciences

MDPI

Article

The Natural Phloroglucinol α-Pyrone Arzanol Protects HaCaT Keratinocytes from Lipopolysaccharide and Polyriboinosinic-Polyribocytidylic Acid-Induced Damage and Promotes Reparative Mechanisms

Franca Piras [1,*], Valeria Sogos [1], Aurora Camola [2], Federica Pollastro [2] and Antonella Rosa [1,*]

[1] Department of Biomedical Sciences, University of Cagliari, 09042 Monserrato, Italy; sogos@unica.it
[2] Department of Pharmaceutical Sciences, University of Eastern Piedmont "Amedeo Avogadro", 28100 Novara, Italy; aurora.camola@uniupo.it (A.C.); federica.pollastro@uniupo.it (F.P.)
* Correspondence: fpiras@unica.it (F.P.); anrosa@unica.it (A.R.)

Abstract

The protective effect of arzanol, a natural prenylated phloroglucinol α-pyrone from the *Helichrysum microphyllum* subsp. *tyrrhenicum*, was investigated in HaCaT keratinocytes exposed to two inflammatory stimuli: lipopolysaccharide (LPS, 0.5–75 μg/mL), a component of gram-negative bacteria, and polyriboinosinic-polyribocytidylic acid (poly I:C, 0.5–50 μg/mL), a synthetic viral RNA analog. LPS and poly I:C significantly decreased HaCaT cell viability (18–93% reduction in the 5–75 μg/mL LPS range and 25% at 50 μg/mL poly I:C, MTT assay) and increased apoptosis and cell death (NucView 488 and propidium iodide assay) after 3 h and 24 h of exposure. Arzanol (1 h of pre-incubation, 5–25 μM) showed a significant protective effect against LPS and poly I:C-induced damage, preserving cell viability (25% of viability increase at 5 μg/mL LPS concentration, and 30% at 50 μg/mL of poly I:C) and decreasing apoptosis/cell death. Western blot analysis demonstrated the ability of arzanol (5 μM) to reduce the apoptotic protein Bax and the inflammatory cytokine IL-1β levels in HaCaT keratinocytes exposed for 3 h to 5 and 10 μg/mL LPS. Moreover, scratch assay showed the arzanol reparative effect on HaCaT cells. Our results qualified arzanol as a protective drug for dermatological applications in human skin diseases.

Keywords: skin; keratinocytes; HaCaT cells; LPS; poly I:C; arzanol; cytotoxicity; apoptosis; proliferation

Academic Editor: Adina Magdalena Musuc

Received: 4 June 2026
Revised: 22 June 2026
Accepted: 25 June 2026
Published: 29 June 2026

1. Introduction

The skin, the largest organ of the body, interacts with both the internal and external environment and is involved in many physiological functions. As a protective barrier, it prevents harmful agents from entering the body and retains essential substances inside. However, its integrity can be easily compromised by external factors, leading to injury, microbial invasion, and inflammation. In response, the skin plays roles in inflammation, forms an innate immune barrier, and engages in reparative wound-healing mechanisms through a complex, highly coordinated biological process [1,2].

Keratinocytes constitute over 90% of the epidermis and undergo a complex, multi-step differentiation process, evolving from a mitotic state to a terminally differentiated form (corneocytes) [3,4]. As the epidermis continuously renews itself, keratinocytes undergo

cornification, a specialized form of programmed cell death distinct from classical apoptosis [4]. During keratinocyte differentiation, apoptosis is not activated, to avoid premature cell death, while caspases (such as caspase-3, -6, -7, and -9) probably remain inactive [4,5]; pro-apoptotic Bax and Bak proteins are induced in the layers of the epidermis [4,5] and several cytokines and growth factors regulate terminal differentiation of keratinocytes [6]. Deregulation of keratinocyte death pathways (including those associated with apoptosis, autophagic cell death, and necrosis) plays a key role in the pathogenesis of various skin diseases [5].

Keratinocytes sense chemical, physical, and microbial agents via distinct toll-like receptors (TLRs), specifically TLR3 and TLR4, that subsequently drive immune responses [2,7,8]. The activation by bacterial products, UV light damage, or chemicals changes the expression of cytokines and chemokines in this epithelial immune system [1,6,7], promoting skin and systemic inflammation [9,10]. Inflammation facilitates the early onset of dermatological disorders, including skin photoaging, psoriasis, pigmented diseases, and skin tumors [10]. Various external agents can induce apoptosis in skin keratinocytes, including cytotoxic drugs (such as chemotherapeutic compounds), toxins, environmental pollutants, UV radiation, and some physiological signals [4,11–13]. These agents trigger a cascade of molecular events that lead to the characteristic features of apoptosis, such as cell shrinkage, DNA fragmentation, and the formation of apoptotic bodies [12,13].

Lipopolysaccharide (LPS), a component of gram-negative bacteria, has been widely used to investigate biological mechanisms, including inflammation and apoptosis, in skin pathologies [10,11,14]. LPS reduces the viability of skin epithelial cells and triggers inflammation, promoting a strong immune response by inducing inflammatory cytokines (such as IL-1, TNF-α, and IL-6) and the expression of various inflammation-related proteins [11,14,15]. The main receptor for LPS in human keratinocytes is toll-like receptor 4 (TLR4), which also plays a role in activating interleukin-1β (IL-1β) in humans [11,14]. LPS can induce apoptosis in skin keratinocytes through various mechanisms, including the activation of inflammatory pathways and the induction of oxidative stress [11,16].

Polyriboinosinic-polyribocytidylic acid (poly I:C) is a synthetic analogue of double-stranded viral RNA and a ligand of toll-like receptor 3 (TLR3) [7,8,17,18]. Skin exposure to poly I:C simulates viral infection, triggering an immune response, primarily through the activation of TLR3, and inflammation, potentially exacerbating skin conditions such as atopic dermatitis [18,19]. The stimulation of TLR3 in skin keratinocytes with poly I:C is a powerful signal for the release of a variety of proinflammatory cytokines [7,11,17,20]. High doses of poly I:C are lethal to keratinocytes, triggering the expression of the proinflammatory cytokines and promoting cytokine release via pyroptosis, a form of cell death mediated by inflammasome activation [21]. Poly I:C can trigger apoptosis in skin keratinocytes through the activation of various intracellular and cell surface receptors (including TLR3), activating downstream signaling pathways (caspases-8, -9, and 3/7) that can lead to programmed cell death [8].

Natural extracts of *Helichrysum italicum*, a Mediterranean species, have long been used to treat skin disorders. This plant possesses a rich and diverse phytochemical profile that confers therapeutic potential through antioxidant, antimicrobial, and anti-inflammatory properties that play essential roles throughout the sequential stages of wound healing [22]. Studies have shown that *H. italicum* extracts can modulate various inflammatory mediators, in particular lowering IL-1β levels, thereby promoting a favorable microenvironment for tissue repair [22].

The natural α-pyrone–phloroglucinol heterodimer arzanol (Figure 1a) has been isolated from the aerial parts of *Helichrysum microphyllum* Cambess. subsp. *tyrrhenicum* Bacch., Brullo & Giusso (synonym of *H. italicum* subsp. *microphyllum*) [23–25], which is endemic

to Sardinia, Corsica, and the Balearic Islands and is used as a dermo-protective plant in traditional medicine [24,25].

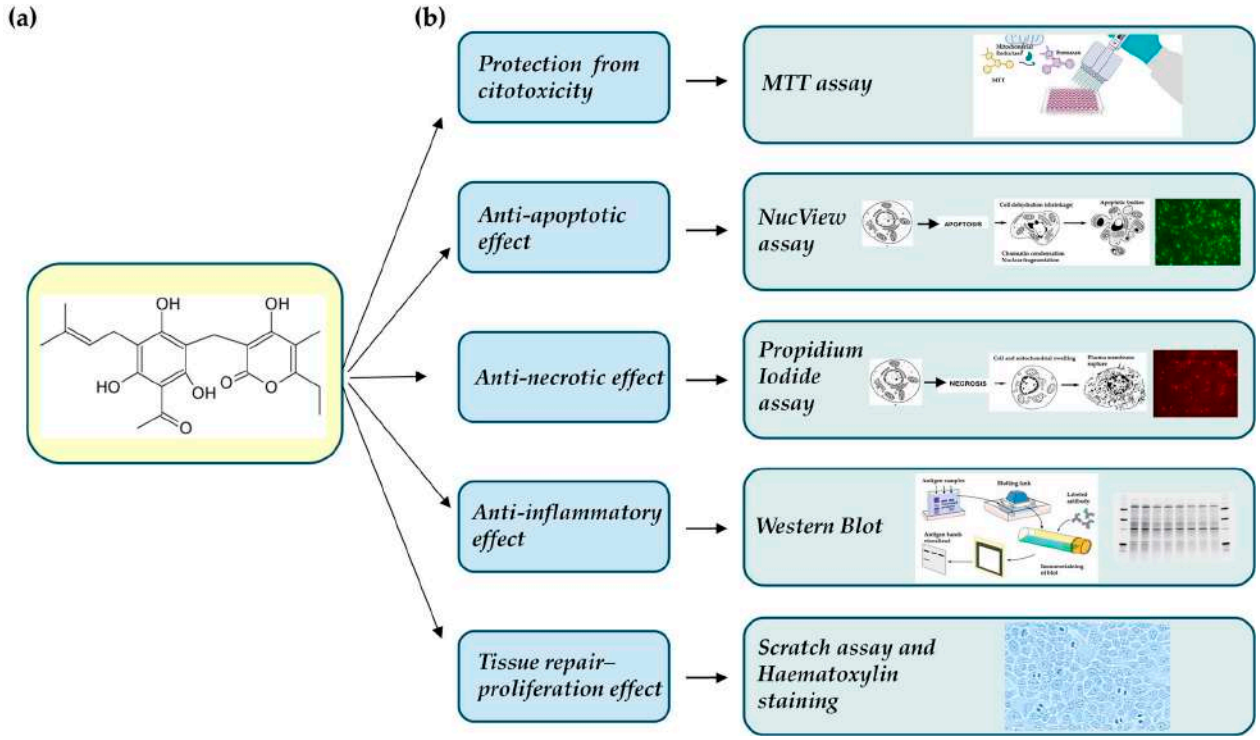

Figure 1. Molecular structure of arzanol (**a**) and scheme of methods applied to evaluate its protective effects in HaCaT cells (**b**).

This phloroglucinol showed anticancer [26,27], antimicrobial [24,28], antioxidant [26,29–33], antiviral [24], and anti-inflammatory activities [24,34,35], as well as positive modulation of brain glycogen phosphorylase activities [36].

Arzanol exhibited radical scavenging activity in various in vitro systems of lipid peroxidation and antioxidant protection in various cell lines and animal models of oxidative stress [26,29–33]. It showed the capacity to inhibit the activation of NF-κB and the release of pro-inflammatory cytokines in LPS-stimulated primary monocytes [24]. Moreover, arzanol also inhibited the biosynthesis of pro-inflammatory lipid mediators like prostaglandin E2 (PGE2) in an in vivo rat model, thus suppressing the inflammatory response of the carrageenan-induced pleurisy [34]. Recently, we demonstrated the ability of arzanol to attenuate cytotoxicity, reactive oxygen species (ROS) production, and mitochondrial membrane depolarization, and to reduce apoptosis in a hydrogen peroxide-induced oxidative stress in keratinocytes [32].

Starting from the pleiotropic effects of arzanol, the current study aimed to extend the knowledge on its role as a natural protective agent for managing cutaneous diseases. For the first time, we explored the ability of arzanol to protect skin keratinocytes against the cell damage induced by the inflammatory agents LPS and poly I:C. The arzanol protection was monitored in terms of its ability to counteract cytotoxicity, apoptosis, and cell death induced by LPS and poly I:C in HaCaT cells, a spontaneously immortalized human keratinocyte cell line obtained from adult skin, that closely resemble normal human keratinocytes and maintain the ability for epidermal differentiation [37]. HaCaT cells are widely used as a robust in vitro model to investigate inflammation, oxidative stress, and cell death triggered by agents such as LPS, H_2O_2, or UV irradiation [6,32,38]. In particular, LPS is a potent inducer of inflammatory damage in HaCaT keratinocytes and stimulates a marked increase

in the production of key inflammatory mediators, such as IL-1β, COX-2, and PGE_2, and a significant reduction in cell viability, ultimately promoting inflammation-driven cell death [11,14].

In addition, we evaluated the involvement of arzanol in tissue repair through a scratch assay, also assessing the mitotic phase. Figure 1b summarizes the protective effects investigated in HaCaT cells and the corresponding experimental approaches.

The results of this work were expected to provide new information on the protective activity of arzanol against inflammatory agent-induced cell damage in human keratinocytes, with potential future dermatological and pharmaceutical applications for skin diseases and other epithelial damage conditions.

2. Materials and Methods

2.1. Materials

Cell culture chemicals and laboratory reagents used in cell culture, including Dulbecco's Modified Eagle's Medium (DMEM, with D-glucose 4.5 g/L), fetal bovine serum (FBS), trypsin 0.25%–EDTA, penicillin, and streptomycin, are all acquired from EuroClone (Pero, MI, Italy). LPS (*Escherichia coli* O26:B6) was purchased from Sigma Aldrich, Merck (Darmstadt, Germany). Polyinosinic-polycytidylic acid (poly I:C) was obtained from InvivoGen (San Diego, CA, USA). Dimethyl sulfoxide (DMSO) and 3-(4,5-dimethylthiazol-2-yl)-2,5-diphenyltetrazolium bromide (MTT) were purchased from Merck Life Science (Milan, Italy). Propidium iodide (PI) was obtained from Thermo Fisher Scientific (Waltham, MA USA), and NucView® 488 (NV) from Biotium (Fremont, CA, USA).

2.2. Arzanol Extraction and Isolation

Arzanol (Figure 1a) was obtained from *H. microphyllum* subsp. *tyrrhenicum*, collected in 2021, Sardinia, Italy, according to literature [24,32]. A plant batch (HM-CA2021 code) [32] was stored in the phytochemistry laboratory of Novara, Italy. Approximately 500 g of dried aerial parts (leaves and flowerheads) were extracted with 2.5 L of acetone in a vertical percolator and filtered under vacuum in a sintered filter to remove the vegetable material [24,29,32]. The acetonic extract was then evaporated at reduced pressure (556 mbar, 40 °C) with a Heidolph Basis He-Vap rotary evaporator (Schwabach, Germany). After solvent evaporation, the obtained gummish residue was dissolved in ethyl acetate (EtOAc)–petroleum ether solution 1:1 to promote arzanol precipitation. Arzanol was characterized by ^{1}H NMR and ^{13}C NMR spectroscopic methods, and the structure was determined by comparing the data with related scientific literature [24,29,32]. The final purity of the arzanol was 98%.

2.3. HaCaT Cell Culture

Human keratinocytes HaCaT cell line was obtained from CLS-Cell Line Services (Eppelheim, Germany). High glucose DMEM (D-Glucose 4.5 g/L) containing 10% FBS, 100 units/mL of penicillin, and 100 µg/mL of streptomycin was used for cell culture. The cells stayed in a water-saturated humidified incubator (37 °C and 5% CO_2). Splitting of the confluent cells was performed once a week by Trypsin 0.25%-EDTA. For experimental studies, HaCaT cells were plated at 10^5/mL density and cultivated to reach almost 80% confluence.

2.4. Effects on Cell Viability

The cytotoxic activities of arzanol, DMSO, LPS, and poly I:C were evaluated by using the colorimetric MTT assay, a method previously used to assess cell viability in HaCaT cells [32]. HaCaT cells were seeded at a density of 10^4 cells/well in a 96-well plate in 100 µL

of complete culture medium and incubated at 37 °C in 5% CO_2 for 48 h. After incubation, the cells (at about 80% confluence) were treated for 24 h with arzanol (5–100 μM, from a 10 mM stock solution in DMSO), DMSO (vehicle, from 0.05 to 1% *v*/*v*), LPS (0.5–75 μg/mL from a 1 mg/mL solution in water), or poly I:C (0.5–50 μg/mL from a 4 mg/mL solution in water) in a fresh medium, whereas control cells (untreated cells) were cultured for 24 h only in a fresh medium. After discharging the medium, the MTT reagent (0.5 mg/mL in DMEM) was added, and the cells were incubated at 37 °C for 3 h as previously reported [32,33]. After the removal of the MTT solution, DMSO was added, and the absorbance of formazan crystals was detected at 570 nm with an Infinite 200 Tecan microplate reader (Salzburg, Austria). The absorbance of control cells was evaluated 100% alive, and viability data were expressed as a percentage of control cells.

The cell morphologies of HaCaT control cells and cells exposed for 24 h to arzanol, DMSO, LPS, and poly I:C, were microscopically observed by ZOE™ Fluorescent Cell Imager (Bio-Rad Laboratories, Inc., Hercules, CA, USA).

2.5. Arzanol Protective Effect Against LPS- or Poly I:C-Induced Damage

The ability of arzanol to protect HaCaT cells from cytotoxic effects induced by LPS and poly I:C cell exposure was determined by employing the MTT assay [32]. Cells were seeded at a density of 10^4 cells/well in 96-well plates in a complete culture medium and incubated for 48 h. Then, HaCaT cells were pre-incubated for 1 h with arzanol (5, 10, and 25 μM) or DMSO (0.5% *v*/*v*, the maximal dose used to dissolve arzanol). Next, the keratinocytes were stimulated for 24 h with LPS (5 and 10 μg/mL) or poly I:C (25 and 50 μg/mL) in fresh medium. Control (untreated) cells were cultured only in fresh medium. After the medium removal, cell viability was evaluated by MTT assay as described above. Viability data were expressed as a percentage of control cells.

The morphologies of control cells, cells exposed to LPS or poly I:C, and cells pre-incubated with arzanol (or the corresponding amount of DMSO) and then exposed to LPS or poly I:C, were evaluated by microscopic observation with a ZOE™ Fluorescent Cell Imager.

2.6. NucView and Propidium Iodide Assays

NucView 488 (NV) and propidium iodide (PI) assays were performed to assess the arzanol protection against apoptosis/cell death caused by LPS or poly I:C in HaCaT cells [32,33]. NV is a non-fluorescent and non-functional complex which involves a fluorogenic DNA dye and a DEVD substrate moiety. Once it is cleaved by caspase-3/7 in the cytoplasm, it releases a high-affinity DNA dye that stains the DNA of the nucleus with green fluorescence, marking apoptotic cells [32,33]. PI, a red fluorescent dye, can pass the altered membrane of injured cells (such as necrotic and late apoptotic cells) and intercalate between DNA base pairs [33].

HaCaT cells were seeded in 96-well plates at 10^4 cells/well in a complete culture medium. Different experimental sets were carried out: control cells, cells pre-incubated for 1 h with arzanol (5 and 10 μM), cells stimulated with 5, 10, and 25 μg/mL LPS, and cells pre-treated with arzanol for 1 h and then exposed to 5, 10, and 25 μg/mL LPS. Then, PI (1 μg/mL final concentration) or NV (5 μL/mL, according to the manufacturer's guidelines) was added to cells and the keratinocytes were incubated, in the dark, for 3 h and 24 h.

Cells were stimulated with poly I:C according to an experimental design analogous to that reported for LPS. HaCaT cells were preincubated with arzanol at 10 and 25 μM concentrations for 1 h and then stimulated with 50 μg/mL poly I:C before the addition of NV or PI dyes and further incubation, in the dark, for 3 h and 24 h, to assess differences

in the antiapoptotic/necrotic effects of arzanol at short and long times of exposure to inflammatory agents.

Microscopic imaging was performed using the ZOE™ Fluorescent Cell Imager, adjusting instrument parameters—offset and gain—according to control cell profiles. Quantitative image analysis was performed using ImageJ (v1.53e), evaluating nearly four PI and NV fluorescence images for each sample. Relative fluorescence intensity was calculated and normalized to control cell values, expressed as a percentage.

2.7. Western Blot Assay

Western blot assay was performed to evaluate the production of inflammatory cytokines such as IL-1β and proapoptotic proteins such as Bax, as previously described [8]. HaCaT cells were pre-incubated for 1 h with 5 μM arzanol and thereafter exposed to LPS (5 and 10 μg/mL) for 3 h. The cells were then lysed with 2% sodium dodecyl sulfate (SDS), ultrasonicated at ice temperature, and centrifuged (10,000× *g*, 10 min). Pierce BCA Protein Assay Kit (Sigma Aldrich, Merck, Darmstadt, Germany) was used to determine the total protein level. After the addition of a loading buffer, samples were heat-denatured by boiling for 5 min. Protein samples (20 μg) were resolved on SDS–polyacrylamide gels, and after being blotted onto PVDF membranes (Hybond-P, Amersham, Marlborough, MA, USA). Non-specific binding on the membrane was blocked with freshly prepared 5% nonfat dried milk in TBST (20 mM Tris-HCl, 150 mM NaCl, 0.1% Tween 20), pH 7.4, for 1 h on a shaking platform at room temperature. The membrane was then incubated at 4 °C overnight with the primary antibodies anti-IL-1β (1:250 dilution, ab9722, Abcam, Cambridge, UK) and anti-Bax (1:1000 dilution; ab32503, Abcam, Cambridge, UK). Once washed, the membrane underwent incubation (room temperature, 1 h) with goat horseradish-peroxidase-conjugated antirabbit IgG (1:10,000 dilution; code 111-035-003 Jackson ImmunoResearch, Ely, UK). Then, the bands were detected by the chemiluminescent substrate Lite a Blot Turbo (Euroclone, Pero, MI, Italy) and visualized by ImageQuant LAS-4000 (GE Healthcare, Little Chalfont, UK). Post-wash, the same membranes were subsequently incubated with anti-GAPDH antibody (1:1000 dilution; Mab 374, Millipore, Merck, Darmstadt, Germany) to normalize protein signal intensity across samples. Band intensity was evaluated using Image Studio software, version 5.2 (LI-COR Biosciences, Lincoln, NE, USA).

2.8. Scratch Assay and Mitotic Index

To assess the potential wound-healing ability of arzanol, a scratch assay was manually performed with a pipette tip on confluent HaCaT cells seeded in 96 multi-wells. Then, the cells were treated with arzanol (10, 25, and 50 μM) for 24 and 36 h, while a subset was maintained as untreated control cells. Then, the cells were fixed with methanol at −20 °C for 4 min, rehydrated in phosphate-buffered saline (PBS), and stained with Carazzi haematoxylin to highlight mitotic figures. Microscopic images were obtained using the ZOE™ Fluorescent Cell Imager, and mitotic counting was performed using ImageJ (v1.53e), evaluating, for each sample, both the full-field cell images and, separately, the cellular region adjacent to the scratch edge. Scratch areas were quantified at 24 h and 36 h from wound induction on at least four images using the ZOE™ Fluorescent Cell Imager. For each time point, the scratch area was delineated and measured, and the percentage of wound closure was calculated relative to the initial scratch area acquired at time 0.

2.9. Statistical Analysis

Initially, the D'Agostino & Pearson test was used to assess the normality of the data distribution using the software package GraphPad Prism version 10.0.0 for Windows (GraphPad Software, Boston, MA, USA). GraphPad Prism was used to estimate the statis-

tical differences between different data groups. Data are presented as mean ± standard deviation (SD) of three or four independent experiments with different replicates. One-way analysis of variance (one-way ANOVA) followed by the Bonferroni multiple comparisons test was used to perform multiple comparisons of the group means. Differences were considered statistically significant when the p-value was less than 0.05.

3. Results

3.1. Impact on HaCaT Cell Viability (MTT Assay)

The cytotoxic effects of arzanol, DMSO, LPS, and poly I:C were assessed using the MTT assay, a widely used method for evaluating cell viability [32,33].

Figure 2 depicts the viability of HaCaT cells (measured as % of control) after incubation for 24 h with different quantities of arzanol (5–100 µM, Figure 2a), LPS (0.5–75 µg/mL, Figure 2b), and poly I:C (0.5–50 µg/mL, Figure 2c).

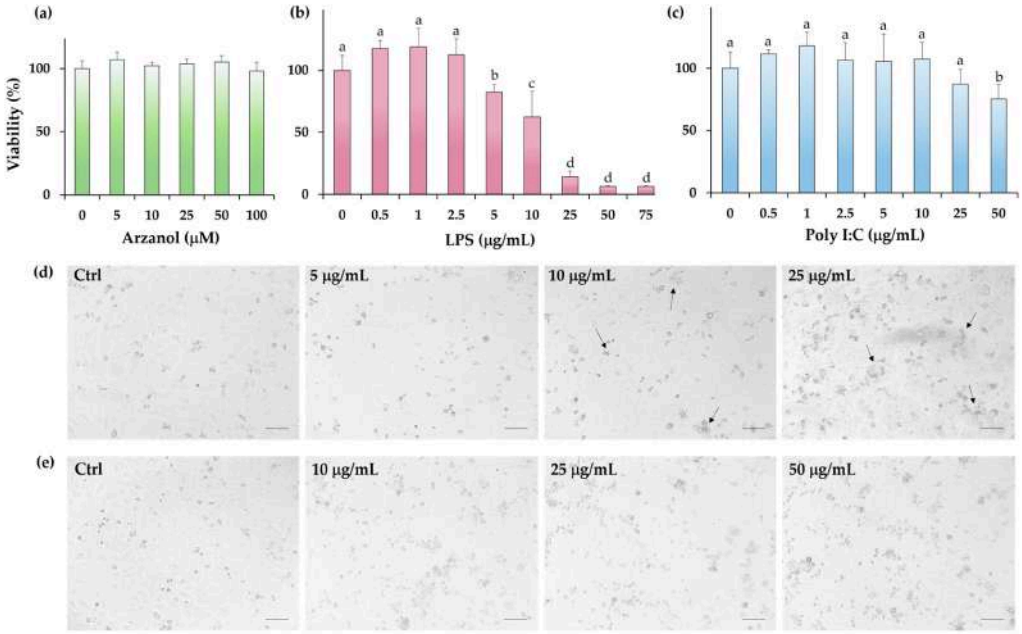

Figure 2. Values of viability (percent of the control, 0) of HaCaT cells, obtained by MTT assay, after incubation for 24 h with arzanol (5–100 µM) (**a**), LPS (0.5–75 µg/mL) (**b**), and poly I:C (0.5–50 µg/mL) (**c**). Three independent experiments were done. Data are given as mean and standard deviation (SD) (n = 15). Arrows indicate cellular fragments, rounded cells, and aggregates. Differences in statistical significance were evaluated by one-way ANOVA and Bonferroni post-test. ^{a,b,c,d}: for all bars with the same letter, their mean values are not statistically different, and if two bars have different letters, their mean values are significantly different ($p < 0.05$). Phase contrast images of HaCaT control cells (Ctrl) and cells stimulated for 24 h with LPS (5, 10, and 15 µg/mL) (**d**) and poly I:C (10, 25, and 50 µg/mL) (**e**). Bar = 100 µm.

Figure 2a shows that the viability of keratinocytes after arzanol incubation was similar to that of the control cells, as previously reported [32]. The vehicle DMSO (0.05–1% v/v), used to dissolve arzanol, did not affect HaCaT cell viability values (24 h of incubation) from 0.05 to 0.5% v/v of DMSO, while a viability reduction of 21% ($p < 0.01$) was determined at DMSO 1% v/v, according to literature [32].

There was a tendency towards increased cell viability after exposure of HaCaT cells to 0.5 to 2.5 µg/mL LPS for 24 h (in the range 112–119%, Figure 2b) when compared with control cells. A significant dose-dependent decrease ($p < 0.001$ versus control cells) in cell viability was observed from the concentration of 5 µg/mL, with values of viability reduction from 18% to 93% in the LPS concentration range of 5–75 µg/mL. The IC_{50} value

(the concentration that decreases the cell viability to 50%) of LPS after 24 h incubation in HaCaT cells was 12.8 μg/mL (by interpolation with a polynomial curve 3rd, $R^2 = 0.9711$).

Keratinocytes did not show a significant change in viability rate when compared with control cells when exposed to poly I:C in the range of 0.5 to 25 μg/mL (Figure 2c), whereas a significant cytotoxic effect ($p < 0.01$ versus control cells) was evidenced at the highest tested concentration (50 μg/mL) of poly I:C, with a cell viability reduction of 25% (IC_{50} value > 50 μg/mL).

Figure 2d shows representative images obtained by phase contrast microscopy of control HaCaT cells and cells treated for 24 h with LPS 5, 10, and 25 μg/mL. A gradual increase, compared with control cells, in cellular fragments, rounded cells, and aggregates was observed in LPS-exposed cells (arrows). An extensive cell damage was observed from LPS 25 μg/mL.

The phase contrast images did not show an evident alteration in cell morphology and density of keratinocytes stimulated with poly I:C in the range of 0.5–5 μg/mL. An increased amount of cellular debris and cell damage was observed in HaCaT cells exposed to poly I:C at 10, 25, and 50 μg/mL (Figure 2e).

Based on the data of cytotoxicity and cell morphology, concentrations of 5 and 10 μg/mL of LPS, and 25 and 50 μg/mL of poly I:C were chosen to assess arzanol's protective effect against their cytotoxicity.

3.2. Arzanol's Protective Effect Against Cytotoxicity Induced by LPS and Poly I:C Stimulation

The MTT assay was used to evaluate the protective effects of arzanol on the decrease in viability induced by LPS or poly I:C stimulation in HaCaT cells.

Figure 3a shows the HaCaT cell viability, expressed as % of the control, measured in control cells, cells stimulated for 24 h with 5 and 10 μg/mL of LPS, and cells pre-incubated for 1 h with arzanol (5, 10, and 25 μM) before LPS exposure.

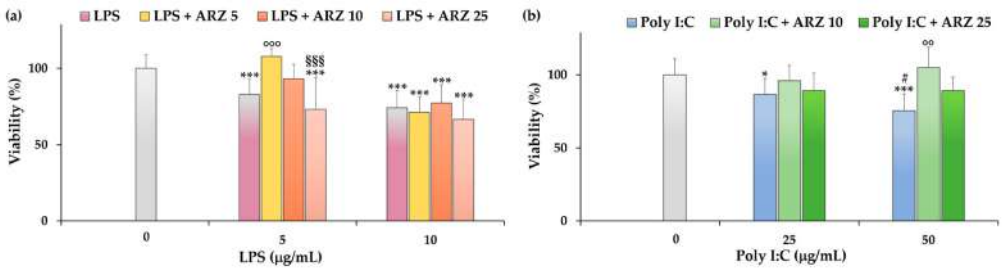

Figure 3. (**a**) Viability of HaCaT cells (MTT assay), expressed as % of the control, measured in control cells (0, grey bar), cells stimulated for 24 h with 5 and 10 μg/mL of LPS, and cells pre-incubated for 1 h with arzanol (5, 10, and 25 μM) before LPS exposure. (**b**) Viability of HaCaT cells (% of the control), measured in control cells (0), cells stimulated for 24 h with poly I:C (25 and 50 μg/mL), and cells pre-incubated for 1 h with arzanol (10, and 25 μM) before poly I:C exposure. Three independent experiments were performed ($n = 15$); data are shown as mean and standard deviation (SD). Differences in statistical significance were evaluated by one-way ANOVA and Bonferroni post-test. *** = $p < 0.001$, and * = $p < 0.05$ versus the respective Ctrl (0); $^{\#}$ = $p < 0.05$ versus poly I:C 25 μg/mL; $^{°°°}$ = $p < 0.001$, $^{°°}$ = $p < 0.01$ versus LPS or poly I:C exposed cells; §§§ = $p < 0.001$ versus LPS + ARZ.

LPS exposure induced a cell viability decrease at both used concentrations, with a viability reduction of 17% at 5 μg/mL and 26% at 10 μg/mL ($p < 0.001$ versus control cells) (Figure 3a). Cell pre-incubation with the lowest arzanol concentration (5 μM) significantly protected against the cytotoxic effect induced by LPS at the dose of 5 μg/mL ($p < 0.001$), while a certain protection was also observed with arzanol at the dose of 10 μM. The protection of arzanol on LPS cytotoxicity decreased with the increase of its concentration.

No protection on viability was observed in cells incubated with LPS 5 and 10 μg/mL and pretreated with arzanol 25 μM (Figure 3a) or 50 μM.

Figure 3b shows the HaCaT cell viability (% of the control), measured in control cells, cells stimulated for 24 with 25 and 50 μg/mL of poly I:C, and cells pre-incubated for 1 h with arzanol (10 and 25 μM) before poly I:C exposure. The exposure to poly I:C markedly reduced HaCaT cell viability, compared with control cells, at 50 μg/mL, with a 14% and 25% reduction in viability at poly I:C 25 and 50 μg/mL, respectively. Pre-incubation with arzanol at 10 μM significantly protected cells from the cytotoxic effect induced by poly I:C at 50 μg/mL, while a lower protection was observed at higher arzanol concentration (25 μM). Arzanol's protective effect was less evident with poly I:C at 25 μg/mL. No protective effect was also observed against the cytotoxicity induced by poly I:C 25 and 50 μg/mL at the arzanol dose of 5 μM.

The range of concentration from 5 to 25 μM was selected to evaluate the protective effect of arzanol in successive experimental models.

3.3. Protective Effect of Arzanol Against Apoptosis and Cell Death

NucView 488 (NV) and propidium iodide (PI) dyes were employed to verify arzanol's protective effect on apoptosis and cell death induced by LPS or poly I:C stimulation in HaCaT cells (Figure 4).

NV fluorescent green dye, a substrate of caspase-3 enzyme, detects the caspase-3/7 activity in cells, whereas the fluorescent red dye PI binds DNA and indicates late apoptotic and necrotic cells [32,33].

Figure 4a shows the phase contrast and green emission (NV) images obtained for HaCaT control cells, cells stimulated for 3 h with LPS (5, 10, and 25 μg/mL), and cells pre-incubated for 1 h with arzanol at doses of 5 and 10 μM alone or before LPS exposure.

Figure 4b reports the NV fluorescence intensity rate, expressed as % control, measured in control HaCaT and LPS-exposed cells with or without arzanol pre-incubation. The LPS stimulation of HaCaT cells determined a significant ($p < 0.001$) increase in the number of green (apoptotic) cells in comparison to control cells at the concentrations of 10 and 25 μg/mL (210% and 180% of control, respectively).

An evident decrease in LPS-induced green fluorescence was observed in keratinocytes pre-incubated with arzanol.

A significant ($p < 0.001$) protective effect against cell apoptosis induced by all LPS concentrations was observed in HaCaT cells pre-incubated for 1 h with arzanol at the doses of 5 and 10 μM.

The cells incubated for 1 h with arzanol alone did not show a significant difference in green NV emission versus control cells.

In Figure 5a, the phase contrast and red emission (PI) images measured for HaCaT control cells, cells stimulated for 3 h with LPS (5, 10, and 25 μg/mL), and cells pre-incubated for 1 h with arzanol at the doses of 5 and 10 μM alone or before LPS exposure are shown.

Figure 5b shows the red fluorescence intensity quantitative data (% of control cells), measured in control HaCaT cells and LPS-exposed cells with or without arzanol pre-incubation. LPS stimulation of HaCaT cells induced an evident increase in IP red fluorescence in comparison to control cells at all tested concentrations. The effect was more marked at LPS 5 μg/mL (fluorescence intensity value of 322%), with a gradual decrease of red fluorescence intensity at LPS 10 μg/mL (269%) and 25 μg/mL (203%).

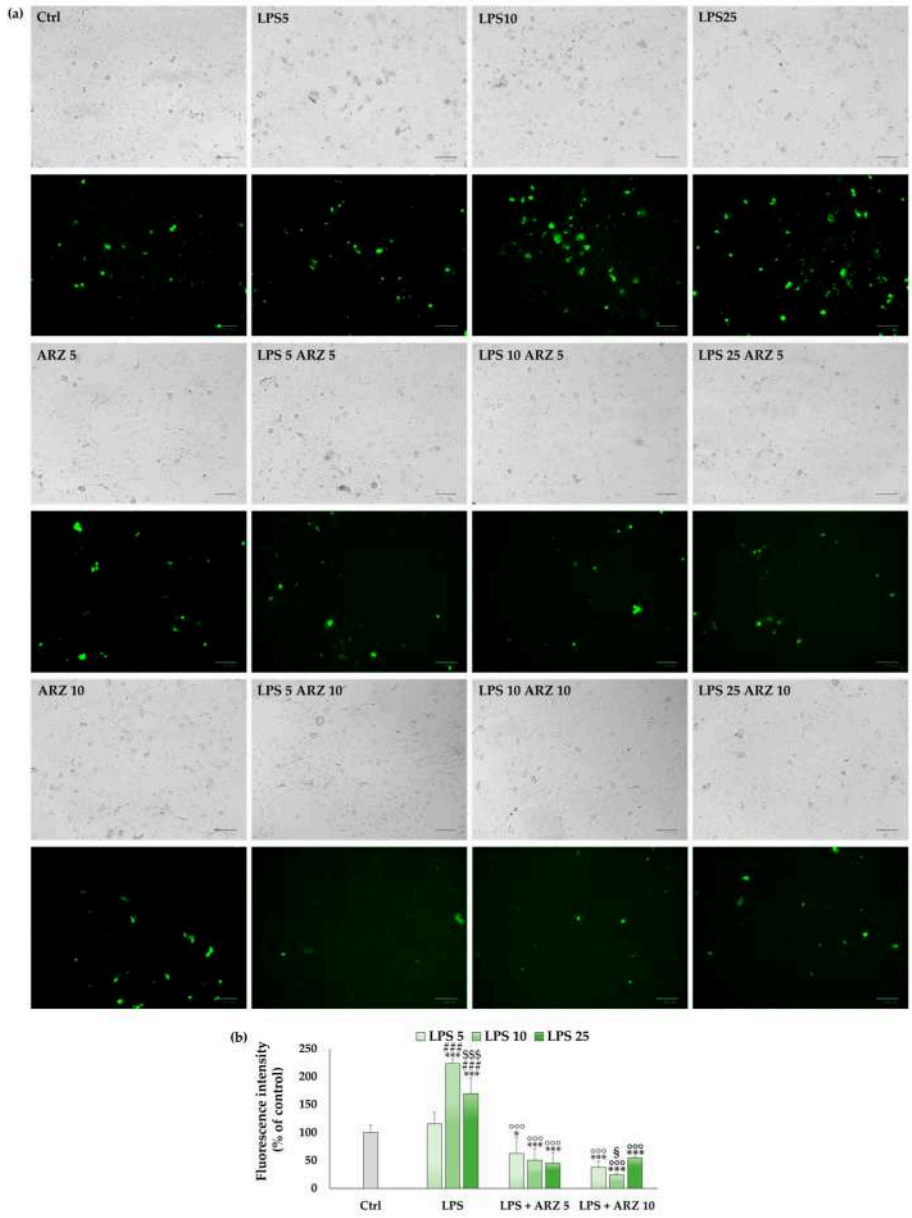

Figure 4. (**a**) Phase contrast images and green emission images (NucView assay) of HaCaT control cells (Ctrl), cells treated with arzanol (5 and 10 μM, 1 h), and HaCaT cells stimulated with LPS (5, 10, and 25 μg/mL, 3 h) in conditions of the presence and absence of arzanol (scale bar = 100 μm). (**b**) Green emission fluorescence intensity (% control intensity) evaluated by image analysis. Three independent experiments were done; results are reported as mean and standard deviation (SD) (n = 12). One-way ANOVA and Bonferroni post-hoc test were performed to explore the statistical significance of differences. *** = $p < 0.001$, * = $p < 0.05$ versus Ctrl; $^{\circ\circ\circ}$ = $p < 0.001$ versus the respective LPS-stimulated cells; § = $p < 0.05$ versus cells pre-treated with arzanol 5 μM. For the LPS group, $^{\#\#\#}$ = $p < 0.001$ versus LPS 5 μg/mL; $^{\$\$\$}$ = $p < 0.001$ versus LPS 10 μg/mL.

Simultaneously, an increase in pyknotic cells and cell debris, and a marked cell depletion were observed in LPS-exposed cells from 5 μg/mL to 25 μg/mL by phase contrast images, which justifies the lower number of red damaged cells observed with the LPS increase. Arzanol pre-treatment (1 h), at both concentrations, showed an evident protective effect against HaCaT cell damage induced by LPS, reducing the red fluorescence intensity versus LPS-stimulated cells (Figure 5b). A marked significant protection against cell death induced by LPS 5 μg/mL was highlighted for arzanol at the doses of 5 and 10 μM ($p < 0.01$

and $p < 0.001$, respectively). The cells incubated for 1 h with arzanol alone did not show a significant difference in red emission versus control cells.

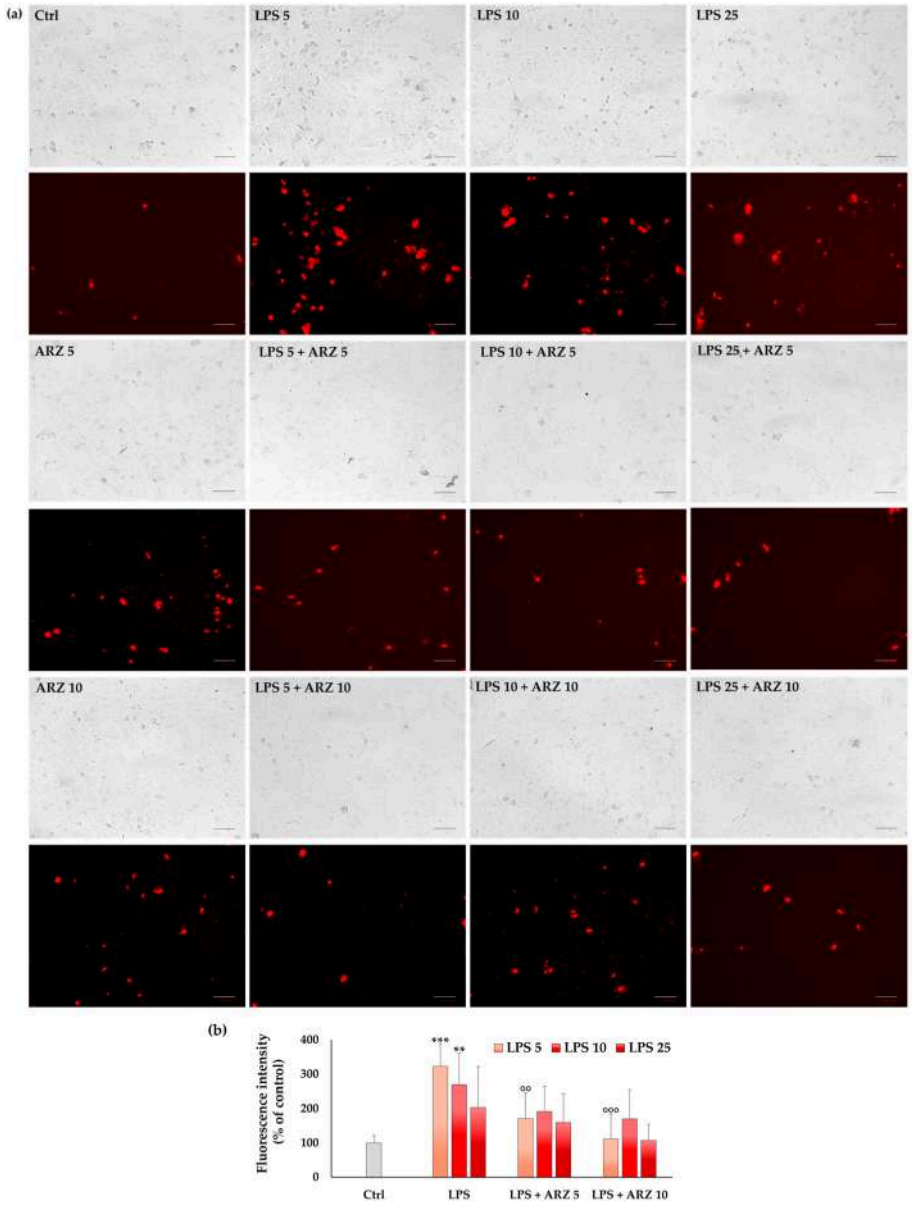

Figure 5. (**a**) Phase contrast images and red emission images (propidium iodide assay) of HaCaT control cells, cells treated with arzanol (5 and 10 μM, 1 h), and HaCaT cells stimulated with LPS (5, 10, and 25 μg/mL, 3 h) with and without arzanol (scale bar = 100 μm). (**b**) Intensity of red emission fluorescence (as % control cell intensity) obtained by image analysis. Three independent experiments were performed; data are shown as mean and standard deviation (SD) (n = 12). The statistical significance of differences was assessed by one-way ANOVA followed by the Bonferroni multiple comparison test. For each series *** = $p < 0.001$, ** = $p < 0.01$ versus the respective control cells (Ctrl); °°° = $p < 0.001$, °° = $p < 0.01$ versus the respective LPS-stimulated cells.

The same experimental design was applied to evaluate the NV green emission and the PI red emission after a long time of exposure (24 h) to LPS (Figure 6).

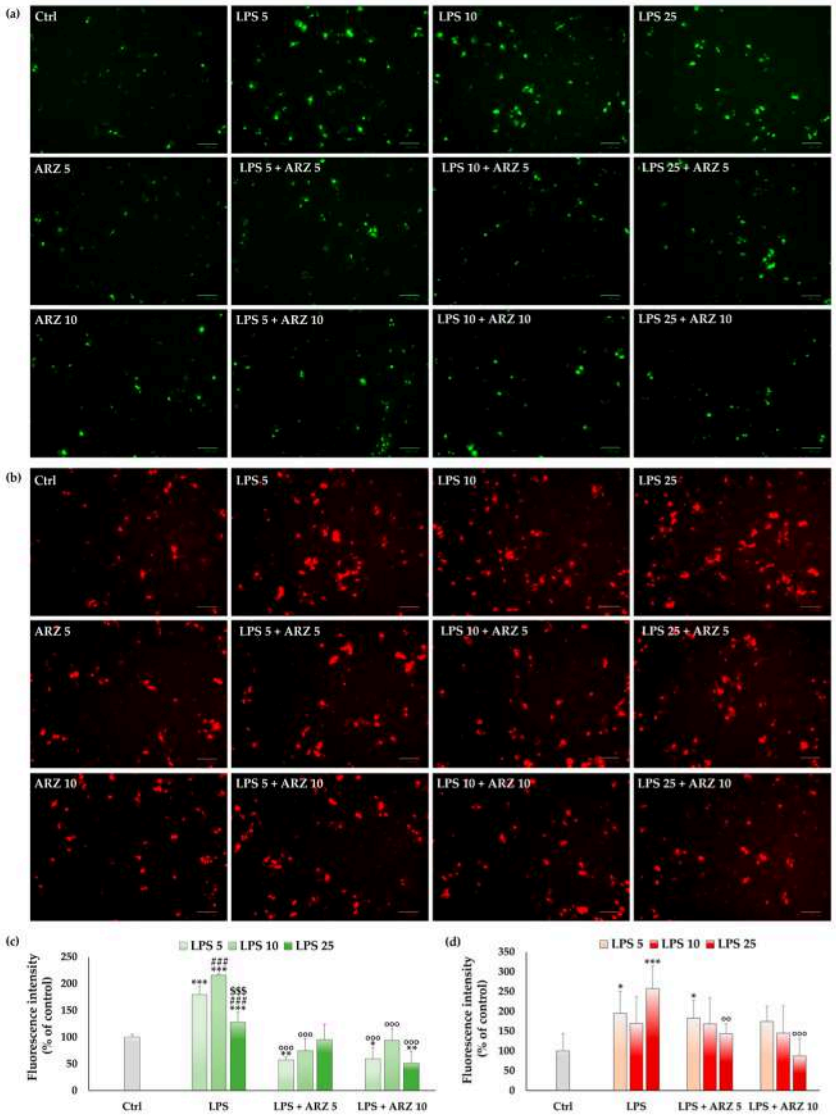

Figure 6. Green emission (NucView assay) images (**a**) and red emission (propidium iodide assay) images (**b**) of HaCaT control cells, cells treated with arzanol (5 and 10 μM, 1 h), and HaCaT cells stimulated for 24 h with LPS (5, 10, and 25 μg/mL) with and without arzanol pre-treatment (scale bar = 100 μm). Fluorescence intensity values of green emission (**c**) and red emission (**d**), measured as % control intensity, obtained by image analysis. Three independent experiments were performed; data are shown as mean and standard deviation (SD) (n = 12). The statistical significance of differences was assessed by one-way ANOVA followed by the Bonferroni multiple comparison test. For each series *** = $p < 0.001$, ** = $p < 0.01$, * = $p < 0.05$ versus the respective control cells (Ctrl); $^{\circ\circ\circ}$ = $p < 0.001$, $^{\circ\circ}$ = $p < 0.01$ versus the respective LPS-stimulated cells. For the LPS group, $^{\#\#\#}$ = $p < 0.001$ versus LPS 5 μg/mL; $^{\$\$\$}$ = $p < 0.001$ versus LPS 10 μg/mL.

HaCaT cell stimulation with LPS 5, 10, and 25 μg/mL, in a similar manner to short-term exposure, induced a significant increase in green fluorescence (apoptotic cells) at all concentrations (Figure 6a,c).

Arzanol 5 and 10 μM significantly ($p < 0.001$) preserved keratinocytes against apoptosis induced by LPS 5 and 10 μg/mL (Figure 6c). Moreover, arzanol 10 μM showed a significant protection against the pro-apoptotic effect induced by LPS 25 μg/mL.

An evident increase in IP red fluorescence, in comparison to control cells, was also observed after 24 h of exposure at all LPS tested concentrations (Figure 6b,d). The protective capacity of arzanol was evident only at 5 and 10 μM ($p < 0.01$ and $p < 0.001$, respectively) against the cell death induced by LPS 25 μg/mL.

Figure 7 shows the phase contrast, green NV emission, and red PI emission images obtained for HaCaT control cells, cells stimulated for 3 h with poly I:C 50 μg/mL, and cells pre-incubated for 1 h with arzanol 10 and 25 μM before poly I:C exposure.

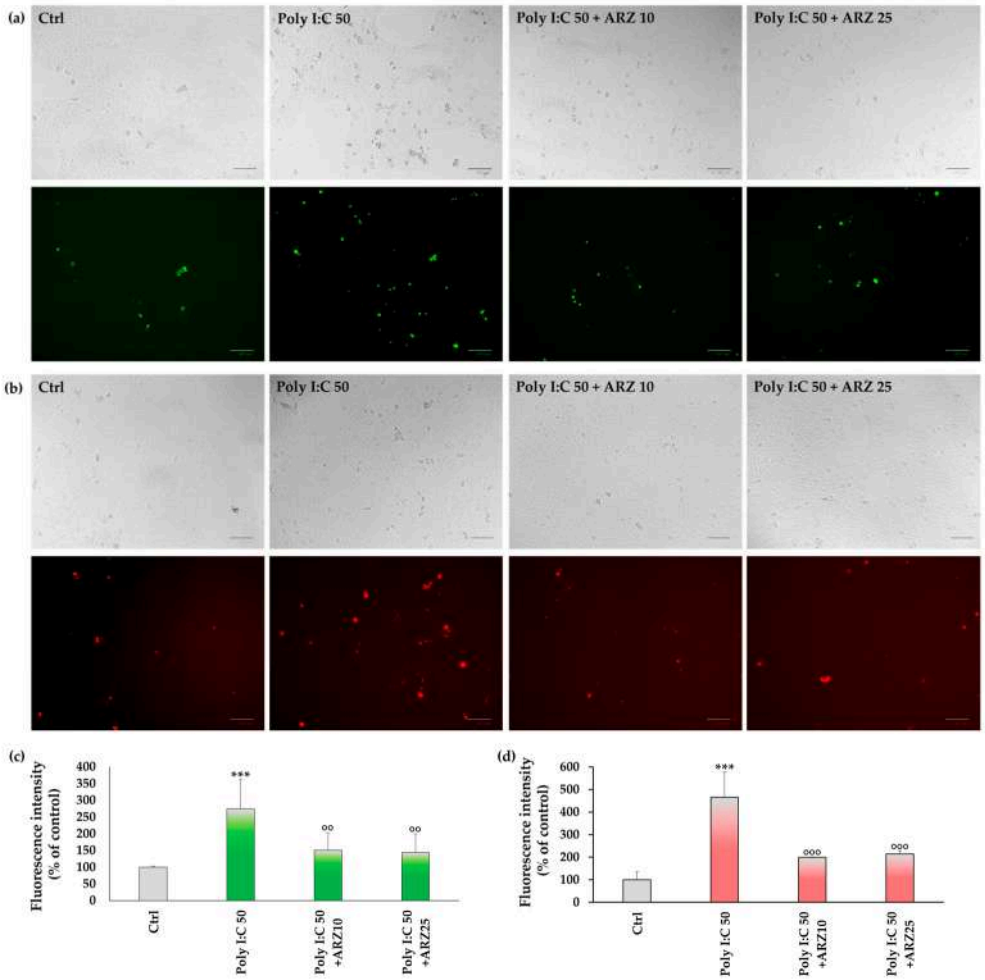

Figure 7. Green emission (NucView assay) images (**a**) and red emission (propidium iodide assay) images (**b**) and respective phase contrast images of HaCaT control cells, HaCaT cells stimulated with poly I:C (50 μg/mL, 3 h), and cells pre-treated with arzanol (10 and 25 μM, 1 h) before poly I:C exposure (bar = 100 μm). Fluorescence intensity values of green emission (**c**) and red emission (**d**), measured as % control cell intensity, obtained by image analysis. Three independent experiments were performed; data are shown as mean and standard deviation (SD) (n = 12). The statistical significance of differences was assessed by one-way ANOVA followed by the Bonferroni multiple comparison test. *** = $p < 0.001$ versus control cells (Ctrl); °°° = $p < 0.001$, °° = $p < 0.01$ versus poly I:C-stimulated cells.

Fluorescence intensity values of green and red emission (measured as % control cell intensity), obtained by image analysis, are reported in Figures 7a and 7b, respectively.

Poly I:C stimulation for 3 h of HaCaT cells induced a significant ($p < 0.001$) increase in the number of green apoptotic cells (275% of green fluorescence intensity) in comparison to control cells (Figure 7c). An important protective effect ($p < 0.01$) against poly I:C-induced apoptosis was observed in HaCaT cells pre-incubated for 1 h with arzanol 10 and 25 μM.

Moreover, the stimulation of HaCaT cells for 3 h with poly I:C 50 μg/mL determined a significantly ($p < 0.001$) higher number of red cells (465% of red fluorescence intensity) in comparison to control cells. Both concentrations of arzanol significantly protected HaCaT cells against cell death induced by poly I:C ($p < 0.001$).

Poly I:C stimulation (50 μg/mL) for 24 h did not induce changes in green fluorescence versus control cells (Figure S1 of Supplementary Materials). Control cells and cells stimulated with poly I:C with or without arzanol pre-incubation (1 h) exhibited similar values of green fluorescence intensity. A slightly significant increase ($p < 0.05$) was observed in red fluorescence after 24 h of exposure to poly I:C 50 μg/mL. Both arzanol concentrations protected HaCaT cells against cell death induced by poly I:C ($p < 0.01$ versus poly I:C-exposed cells for arzanol 25 μM).

The vehicle DMSO, used to dissolve arzanol, did not show any effect against LPS- or poly I:C-induced stimulation at 3 h and 24 h by NV or PI assay, with values similar to control cells.

3.4. Arzanol Activity on Bax and IL-1β Proteins

We profiled the changes in expression levels of Bax and IL-1β proteins in HaCaT cells following arzanol treatment to confirm the involvement of the anti-apoptotic and anti-inflammatory effect of arzanol in the LPS-induced damage. The lowest tested concentration of arzanol (5 μM), which produced a protective effect across assays, was selected for Western blot analysis to investigate molecular mechanisms under physiologically relevant conditions.

Figure 8a,b show the levels of Bax and IL-1β, respectively, measured by Western blot analysis in control HaCaT cells, cells stimulated for 3 h with LPS 5 and 10 μg/mL, and cells pre-treated for 1 h with arzanol 5 μM alone and before LPS exposure.

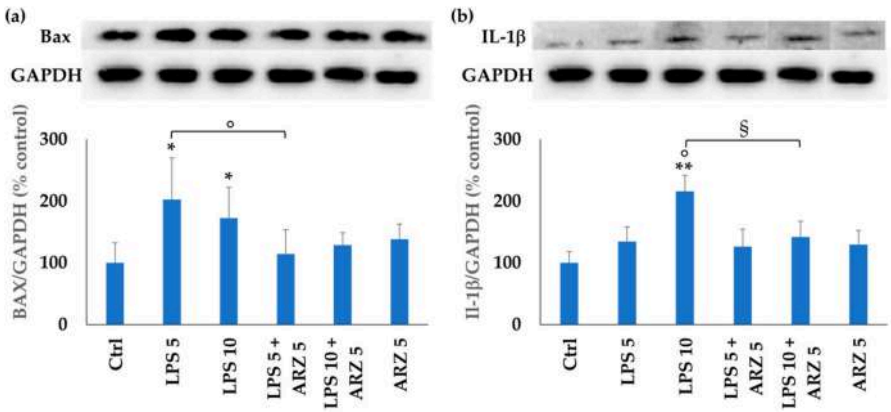

Figure 8. Expression level measured by Western blot analysis of Bax (**a**) and IL-1β (**b**) proteins in HaCaT control cells (Ctrl), cells stimulated for 3 h with LPS (5 and 10 μg/mL), and cells pre-treated for 1 h with arzanol 5 μM alone and before LPS exposure. Protein expression levels of Bax and IL-1β in control and treated HaCaT keratinocytes were quantified by densitometric analysis and normalized to GAPDH as a loading control. Data are reported as the mean and standard deviation (SD) of three different experiments ($n = 3$). One-way ANOVA and the Bonferroni multiple comparison test were performed to explore the statistical significance of differences. ** = $p < 0.01$, * = $p < 0.05$ versus Ctrl cells; ° = $p < 0.05$ versus cells exposed to LPS 5 μg/mL; § = $p < 0.05$ versus cells exposed to LPS 10 μg/mL.

Bax (Figure 8a) and IL-1β (Figure 8b) protein levels in the control and treated HaCaT cells were quantified and normalized to the loading control glyceraldehyde-3-phosphate dehydrogenase (GAPDH) by densitometry.

The exposure to both LPS concentrations induced a significant increase ($p < 0.05$ versus control cells) in the HaCaT cell level of the apoptotic protein. Pre-treatment with arzanol 5 μM before LPS stimulation induced a significant ($p < 0.05$) decrease in Bax level versus cells exposed to LPS 5 μg/mL, but no significant protection was observed at LPS 10 μg/mL. A significant increase ($p < 0.01$ versus control cells) in the HaCaT cell level

of the inflammatory cytokine IL-1β was only found after exposure to LPS 10 μg/mL. A significant ($p < 0.05$) decrease in IL-1β level versus cells exposed to LPS 10 μg/mL was found in keratinocytes pre-treated with arzanol 5 μM. HaCaT cells pre-treated for 1 h with arzanol 5 μM alone did not show differences in Bax and IL-1β protein levels versus control cells.

3.5. Scratch Assay and Mitotic Index

Figure 9 shows the contrast phase images of the scratch areas (Figure 9a) and the values of % closure (Figure 9b) determined in control HaCaT cells and arzanol-treated cells at time 0, 24, and 36 h post scratch induction.

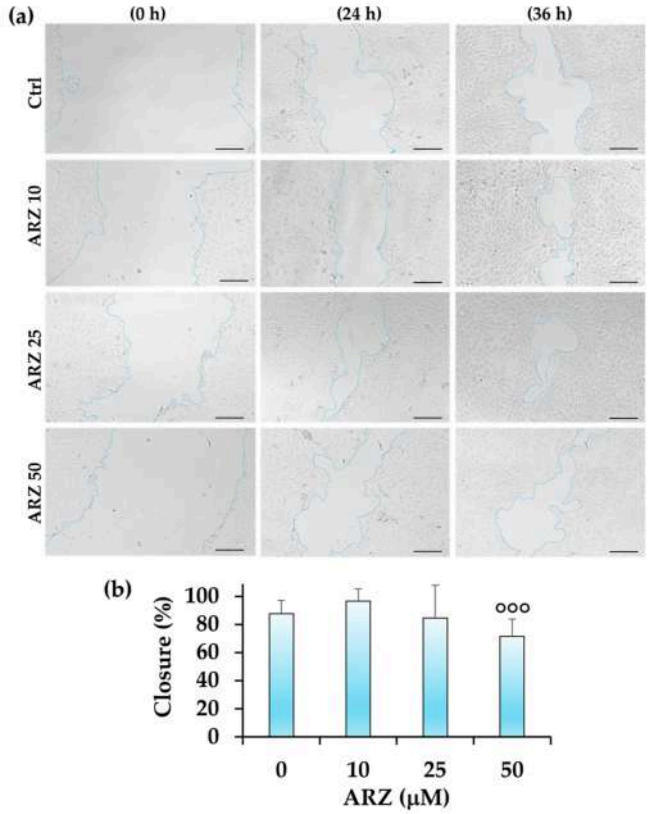

Figure 9. Contrast phase images of the scratch areas (**a**) and the percentage of closure (**b**) determined at 0, 24, and 36 h post scratch induction in control HaCaT cells (Ctrl, 0) and cells incubated for 36 h with different arzanol concentrations (10, 25, and 50 μM). Areas were quantified using ImageJ software on at least 4 images for each experiment (bar = 100 μm). Data are reported as the mean and standard deviation (SD) of four different experiments ($n = 8$). One-way ANOVA and the Bonferroni multiple comparison test were performed to explore the statistical significance of differences. ^{ooo} = $p < 0.001$ versus 10 μM arzanol.

After 24 h, no significant differences in the percentage of wound closure were detected between control and treated samples. At 36 h, however, the treatment with arzanol 10 μM produced a clear reparative effect, showing 96% closure, although one that was not statistically significant when compared with the control (87% closure) (Figure 9b). The % of closure induced by arzanol 25 μM (85%) was similar to that measured in control cells.

Haematoxylin staining was used to verify the proliferative effect of arzanol in HaCaT cells 24 h after the mechanical damage (scratch). Figure 10 shows the contrast phase images of the scratch front regions (Figure 10a) and mitotic index quantified in the scratch front areas and in the distant regions (Figure 10b) measured in HaCaT control cells and cells incubated for 24 h with different arzanol concentrations (10, 25, and 50 μM).

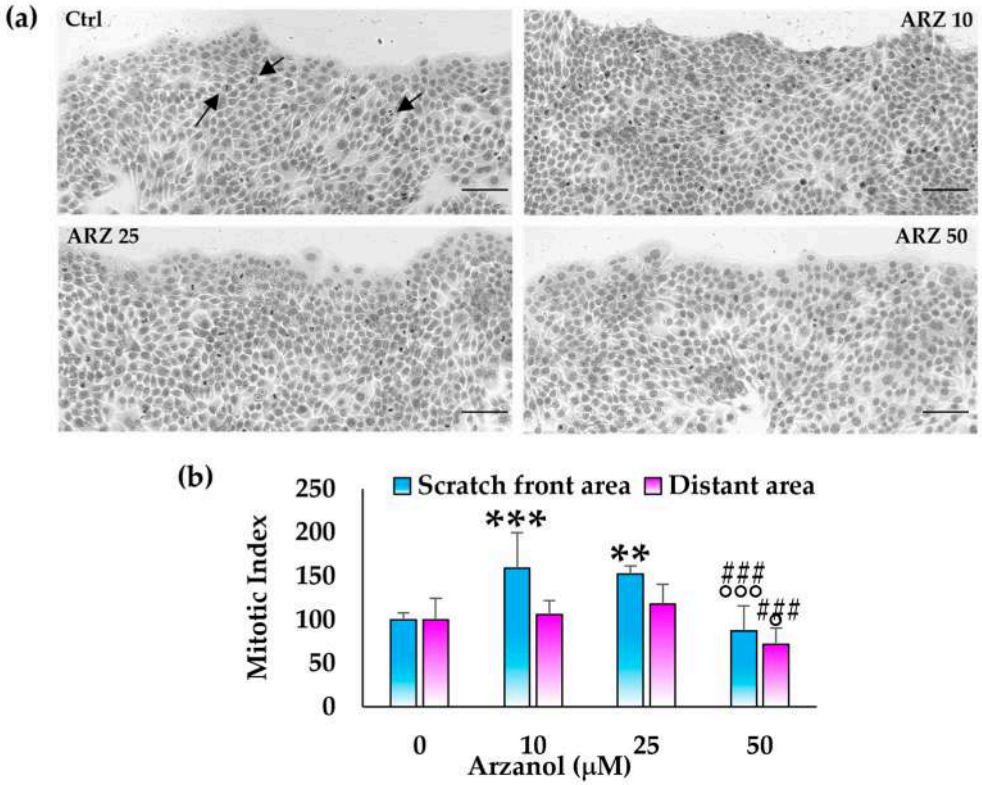

Figure 10. Contrast phase images of the scratch front regions (**a**) and mitotic index quantified in the scratch front areas and in the distant regions (**b**) 24 h after the scratch in control HaCaT cells (Ctrl, 0) and cells incubated for 24 h with different arzanol concentrations (10, 25, and 50 μM). Mitoses were highlighted with haematoxylin, quantified using ImageJ software, and normalized to cell area from at least four images (bar = 100 μm). Arrows indicate some mitotic figures. Data are reported as the mean and standard deviation (SD) of four different experiments (n = 8). One-way ANOVA and the Bonferroni multiple comparison test were performed to explore the statistical significance of differences. *** = $p < 0.001$, ** = $p < 0.01$ versus Ctrl cells; ^{ooo} = $p < 0.001$, ^{o} = $p < 0.05$ versus 10 μM arzanol; $^{###}$ = $p < 0.001$ versus 25 μM arzanol.

At 24 h after scratching and incubation in arzanol at different concentrations, the number of mitotic figures was evaluated in the cell layer (approximately 15–20 cell lines) adjacent to the leading edge and in regions distant from the wound.

In Figure 10a, mitotic figures are visible in the areas behind the scratch front but not at the leading edge, which shows cells with nuclei containing finely dispersed chromatin and expanded cytoplasm. The number of mitotic figures, normalized to the analyzed area, was significantly higher in cells treated with arzanol 10 μM (159%) and 25 μM (152%) than in the control cells. At arzanol 50 μM, the number of mitotic figures was similar to that of control cells. Moreover, when comparing the scratch front with distant areas, the number of mitotic figures was greater in regions adjacent to the scratch front than in those farther away.

4. Discussion

The skin, the largest organ of the body, and one that continuously self-renews, represents the first protective barrier of an organism against external physical, chemical, and biological insults, including wounding, ultraviolet (UV) radiation, and microorganisms, and plays a crucial role in host defense mechanisms [4,6,32]. Exposure to external insults changes the skin oxidative balance, triggering inflammation and accelerating the onset of dermatological conditions, including photoaging, psoriasis, pigmentary disorders, and skin tumors [10].

Beyond their structural and barrier roles in the epidermis, keratinocytes actively participate in the regulation of skin inflammation, immune surveillance, and tissue repair [4]. In vitro studies using cultured human keratinocytes, such as HaCaT cells, are widely utilized to investigate the cellular mechanisms underlying persistent skin inflammation and oxidative stress-related conditions [6,32,39–41].

We recently demonstrated that arzanol, a naturally occurring prenylated phloroglucinyl α-pyrone, can protect skin HaCaT keratinocytes against H_2O_2-induced oxidative damage [32]. This study aimed to extend the knowledge on the protective effect of arzanol against skin injury conditions. We explored, for the first time, the ability of arzanol to protect skin keratinocytes against the cell damage induced by the inflammatory agents LPS and poly I:C. The bacterial endotoxin LPS and the synthetic viral RNA poly I:C are often used in cell models to mimic the pathological process caused by bacteria and viruses, respectively [42].

Preliminarily, the cytotoxic effect of arzanol was assessed by MTT assay to identify the non-toxic concentrations in keratinocytes. In our experimental conditions, arzanol demonstrated no toxicity toward HaCaT cells after 24 h of incubation in the range 0.5–100 μM as previously reported [32]. This range of concentrations was selected based on previous data on arzanol cytotoxicity in other normal cell lines [26,29,30,34]. This α-pyrone has been demonstrated to be generally well tolerated in normal cells, exhibiting no cytotoxic effects in an immortalized Vero cell line (in the range of 0.5–50 μM after 24 h of incubation) [29,30], peripheral blood mononuclear cells (at 10 and 30 μM, 24 h of incubation) [34], and differentiated CaCo-2 cells as a model of the intestinal epithelium (in the range of 5–100 μM, 24 h of incubation) [26,30]. Then, concentrations of 5, 10, and 25 μM of arzanol were selected to evaluate its protective effect against the injury conditions induced by the inflammatory agents LPS and poly I:C. These concentrations of arzanol were physiologically relevant because they have been previously demonstrated to exhibit antioxidant and anti-inflammatory properties in various cell models, without causing significant cell death [24,29,30,33].

LPS comprises a major part of the outer membrane of gram-negative bacteria and can induce a strong inflammatory response, activating various cell types, including epithelial cells [10,11,14,16,42,43]. LPS activates toll-like receptors (TLRs), expressed by cells of the innate immune system, and specifically binds to TLR4, inducing apoptosis or other forms of cell death [11,14,16,42–45]. TLR4-mediated apoptosis is a complex process that can lead to NF-κB activation and production of inflammatory cytokines (like TNF-α, IL-1β, and IL-6), chemokines, and reactive oxygen species (ROS) [11,43,44]. LPS-induced generation of ROS has been demonstrated to activate apoptotic proteins, including Bax [46,47]. TLR4 is present in the keratinocytes of normal human epidermis in vivo and in HaCaT cells [48,49].

Our results show that exposure for 24 h with LPS induced a significant decrease in HaCaT cell viability (MTT assay) from 5 μg/mL, with an IC_{50} value of 12.8 μg/mL. A gradual increase in cell damage and the quantity of cellular fragments had already been observed by phase contrast microscopy after a short period of exposure (3 h) of HaCaT cells to LPS (5–25 μg/mL), coupled with a significant increase in the number of green apoptotic and red dead cells (NV and PI assays, respectively). An evident increase in the green and red fluorescence (apoptosis and cell death, respectively) was also observed after 24 h of exposure to LPS. NV dye, an enzyme caspase-3 substrate, is capable of detecting the activity of caspase-3/7 within cells, staining the DNA of the nucleus with green fluorescence, and then marking apoptotic cells [32,33]. PI is a DNA-binding fluorescent red dye able to highlight cells with compromised plasma membranes (injured/dead cells), including late apoptotic cells, necrotic cells, and cells derived from pyroptosis [32,33,50].

According to our results, previous studies showed that LPS reduced HaCaT cell viability and induced apoptosis [11,14]. A time- and dose-dependent decrease in cell viability (by MTT assay) has previously been reported in HaCaT cells exposed to LPS, with approximately 40% of cell viability reduction when keratinocytes were treated with 1 μg/mL LPS for 24 h [14]. Moreover, HaCaT cells exposed for 24 h to LPS (1 μg/mL) showed a noteworthy increase (three times greater than control cells) in the number of apoptotic cells stained with annexin V-FITC/PI and analyzed by flow cytometry [14]. A previous study reported a significant cell viability reduction in human HaCaT keratinocytes exposed for 24 h to 25 or 50 μg/mL LPS (16.9 and 27.14%, respectively) compared with the control cell group [11]. Another study reported the cytotoxic effect of LPS 1 μg/mL (24 h of exposure) in HaCaT keratinocytes, coupled with a marked apoptosis induction [15].

The preincubation (1 h) with arzanol 5 μM exhibited a significant protective effect against the rate of cytotoxicity induced in HaCaT cells by LPS at the dose of 5 μg/mL, with a lower protection at 10 μM. We previously demonstrated the capacity of arzanol (24 h of pre-incubation) to counteract the cytotoxicity induced in HaCaT keratinocytes by the exposure to hydrogen peroxide 2.5 and 5 mM for 2 h [32].

Arzanol, at the doses of 5 and 10 μM, significantly protected HaCaT cells against apoptosis and cell death (evaluated by NV and IP assays, respectively) induced by LPS at both times of exposure (3 h and 24 h). Some differences in the arzanol protective action emerged in relation to the LPS amount and time of exposure. A previous study has evidenced the ability of arzanol (50 μM) to preserve keratinocytes against the pro-apoptotic effect of hydrogen peroxide at doses of 2.5 and 5 mM [32].

The results demonstrate the protective role of arzanol from LPS-induced cellular damage in HaCaT keratinocytes. A previous study highlighted its ability (at 5–25 μM) to inhibit the activation of NF-κB and the release of pro-inflammatory cytokines in LPS-stimulated human peripheral monocytes, with a potent inhibition of the production of IL-1β and TNFα (IC_{50} values = 5.6 and 9.2 μM, respectively), qualifying it as a potent plant-derived anti-inflammatory chemotype [24].

Poly I:C is a synthetic analogue of double-stranded RNA typically found in some viruses and activates toll-like receptor 3 (TLR3) [7,8,17,18,42]. Keratinocytes express high levels of TLR3 [42]. The TLR3 stimulation induced by poly I:C in primary human adult keratinocytes (HEKa) has been demonstrated to induce cytotoxicity, the release of pro-inflammatory cytokines, and pyroptotic and apoptotic cell death [8]. The activation of the apoptotic caspases -8, -9, and -3/7 was evidenced in keratinocytes after TLR3 stimulation induced by poly I:C [8].

In our experimental conditions, poly I:C emerged as less cytotoxic in HaCaT cells than LPS in the range of 5 to 50 μg/mL after 24 h of exposure. The exposure for 24 h to poly I:C led to a significant decrease in HaCaT cell viability only at 50 μg/mL. However, a certain increase in the level of cellular debris and cell damage was observed from 10 μg/mL of poly I:C after 24 h of exposure by phase contrast microscopy. Poly I:C stimulation (at 50 μg/mL) of HaCaT cells for 3 h induced a significant increase in the number of apoptotic and dead cells (NV and PI assays, respectively). Whereas a significant increase, versus control cells, of red fluorescent cells was only observed after 24 h exposure to poly I:C.

Literature data evidenced the capacity of poly I:C to affect HaCaT cell viability; however, the extent of this effect emerged as related to poly I:C concentration and its combination with other treatments [17,51]. According to our data, a previous study has shown that stimulation of HaCaT cells for 24 h with poly I:C in serum-free DMEM did not affect cell viability in the dose range of 1.25–20 μg/mL [7]. A significant viability reduction (approximately 25% versus control cells) was previously reported after 72 h of incubation

of HaCaT keratinocytes with poly I:C at the dose of 1 μg/mL [17]. Moreover, poly I:C has been reported to induce apoptosis and necroptosis in HaCaT cells [51].

Our results show that pre-incubation for 1 h with arzanol 10 μM significantly protected the cells from the cytotoxic effect induced by poly I:C 50 μg/mL, while a lower protection was observed at 25 μM. Moreover, arzanol, at both tested concentrations (10 and 25 μM), significantly counteracted apoptosis and cell death induced by poly I:C after 3 h of exposure. A protective effect of arzanol against late apoptosis and cell death was also observed in HaCaT keratinocytes after 24 h of exposure to poly I:C 50 μg/mL (PI assay). A previous study evidenced the arzanol inhibition of HIV-1 replication in T lymphocytes, qualifying it as a potent antiviral chemotype [24].

Taken together, our data demonstrate the ability of arzanol to preserve HaCaT cells from the damage (cytotoxicity, apoptosis, and cell death) induced by the inflammatory agents LPS and poly I:C (as a model of bacterial and viral infection, respectively), through its well-recognized diverse biological activities (anti-inflammatory, antioxidant, and antiviral properties).

Subsequently, we explored, via Western blot analysis, the ability of arzanol to reduce the activation of Bax protein, an apoptotic marker [45,46,52,53], and IL-1β, an inflammatory marker [11,44], both of which have previously been demonstrated to be implicated in LPS-induced injury. We selected the lowest concentration of arzanol (5 μM) that produced a protective effect across assays. This minimal effective dose allowed us to investigate molecular mechanisms under physiologically relevant conditions.

A higher expression of Bax and IL-1β proteins was measured in LPS-stimulated HaCaT cells (after 3 h of exposure) with respect to control cells. Arzanol preincubation (1 h) at 5 μM before LPS stimulation significantly decreased Bax level versus cells exposed to LPS 5 μg/mL and IL-1β level versus cells exposed to LPS 10 μg/mL. We demonstrated the ability of arzanol to preserve human skin HaCaT keratinocytes against the LPS-induced damage by interfering with Bax production and then with Bax-mediated apoptosis. IL-1β is an inflammatory cytokine that follows NF-κB activation [23,34]. Our results confirm the ability of arzanol to reduce the pro-inflammatory mediator IL-1β, maybe through its capacity to act as an NF-κB inhibitor, as previously demonstrated in LPS-stimulated human peripheral monocytes [24,35].

The protective effect of arzanol on the production of inflammatory (IL-1β, IL-6, NF-κB), pro-apoptotic (Bax and caspase enzymes), and cell-cycle markers in HaCaT cells at different times of exposure to LPS will be the focus of our next study to provide a more comprehensive understanding of the protective mechanism of arzanol.

In addition, we investigated the potential role of arzanol in wound healing. Skin wound healing is a multifaceted biological process that remains only partially understood. It progresses through three partially overlapping phases: inflammation, proliferation, and tissue remodeling [54]. Cell divisions are essential for proper wound repair, so we had a specific focus on monitoring the arzanol effect on the proliferative phase.

In skin wounds, three distinct regions can be identified: the leading edge, the proliferative hub, and the adjacent healthy tissue [54]. The leading edge contains no proliferating cells; instead, these cells actively migrate into the wounded area to promote wound closure [55]. In contrast, the proliferative hub is expected to contain numerous cells undergoing mitosis [56]. In our samples, mitotic figures were quantified within the ~20-cell-wide layer adjacent to the scratch front, which consistently showed, at 24 h after scratch induction, a higher number of mitoses than regions located farther from the wound edge, likely corresponding to the proliferative hub. This zone also displayed a consistently greater mitotic enrichment in arzanol-treated cells compared with untreated controls, exceeding the levels observed in more distal areas. The number of mitotic figures was significantly

higher in cells treated with 10 and 25 μM arzanol compared with control cells, whereas at 50 μM it returned to control levels. This trend is consistent with the biphasic behavior often observed with phenolic compounds, which can stimulate cellular defense mechanisms at low concentrations and lose this stimulatory activity as the dose increases [57]. Accordingly, arzanol appears to elicit a biphasic response: low concentrations promote a beneficial response with pro-proliferative effect, reflected by an increased mitotic index, while at 50 μM the proliferative activity simply returns to baseline, without evidence of cytotoxicity.

Moreover, measurement of the scratch area revealed a greater degree of closure in samples treated with 10 μM arzanol compared with the control. Proper wound repair depends on a finely balanced interplay between the beneficial and harmful actions of ROS. An early ROS burst is required to initiate the repair program, whereas sustained or excessive ROS production becomes detrimental. Persistent oxidative stress—driving lipid peroxidation, protein modification, and DNA damage—impairs healing by promoting apoptosis and cellular senescence [58]. Our previous work showed that arzanol exerts antioxidant and anti-apoptotic effects in HaCaT cells, both under H_2O_2-induced oxidative stress and in basal conditions [32]. Taken together, these observations suggest that, during an acute insult such as a scratch, the ability of arzanol to modulate ROS levels may help establish a microenvironment that supports cell proliferation.

This study has limitations, and further research is needed to translate the findings into real physiological contexts, determine the duration of arzanol's protective effect, and provide insights into pathways relevant to skin inflammation, anti-inflammatory responses, and various forms of cell death, such as apoptosis, expanding the protein and transcriptional analysis. The absence of the flow cytometry technique represents a limitation of the present work; therefore, future studies will include it to obtain rigorous quantitative measurements of early and late apoptosis. Moreover, the role of arzanol in wound healing requires deeper study. As HaCaT cells are an immortalized cell line whose physiological state may differ from that of primary keratinocytes, further investigations employing primary keratinocytes or in vivo approaches are necessary to enhance clinical applicability.

5. Conclusions

There is a growing interest in using naturally derived compounds to treat skin diseases due to their potential efficacy and limited side effects compared with conventional treatments. The natural α-pyrone–phloroglucinol heterodimer arzanol, isolated from the aerial parts of *H. microphyllum* subsp. *tyrrhenicum*, has demonstrated pleiotropic biological activity. In this study, we highlighted the protective effects of arzanol against cell injury induced in HaCaT keratinocytes by LPS and poly I:C, which are molecules able to simulate bacterial and viral infection, respectively, and which are widely used to induce inflammatory effects in cellular models.

Arzanol showed a significant protective effect against HaCaT cell damage induced by these inflammatory agents, preserving cell viability and decreasing apoptosis and cell death. Moreover, the reduction of the production of the inflammatory cytokine IL-1β and the apoptotic protein Bax was evidenced as being crucial for protecting HaCaT keratinocytes against LPS-induced damage. Arzanol treatment was performed as a pre-treatment prior to exposure to the damaging stimuli, enabling the assessment of its potential preventive activity. By attenuating early inflammatory signaling and limiting apoptosis and viability reduction, arzanol may establish a cytoprotective baseline state in keratinocytes, thereby reducing their susceptibility to subsequent stress-induced damage. In addition, arzanol, by supporting cell proliferation, could potentially enhance wound healing.

Our results qualified arzanol as a potential protective drug for dermatological applications in human skin diseases.

Supplementary Materials: The following supporting information can be downloaded at https://www.mdpi.com/article/10.3390/app16136472/s1, Figure S1: Contrast phase, green fluorescence (NV assay) images and % of green fluorescence intensity of HaCaT cells pre-treated with arzanol and cells stimulated for 24 h with poly I:C; Figure S2: Contrast phase, red fluorescence (PI assay) images and % of red fluorescence intensity of HaCaT cells pre-treated with arzanol and cells stimulated for 24 h with poly I:C.

Author Contributions: Conceptualization, F.P. (Franca Piras) and A.R.; methodology, F.P. (Franca Piras) and V.S.; formal analysis, F.P. (Franca Piras) and A.R.; investigation, F.P. (Franca Piras); resources, V.S.; data curation, F.P. (Franca Piras) and A.R.; writing—original draft preparation, F.P. (Franca Piras) and A.R.; writing—review and editing, V.S., A.C., and F.P. (Federica Pollastro); visualization, F.P. (Franca Piras) and A.R. All authors have read and agreed to the published version of the manuscript.

Funding: This research received no external funding.

Institutional Review Board Statement: Not applicable.

Informed Consent Statement: Not applicable.

Data Availability Statement: The data that support the findings of this study are available from the corresponding author upon reasonable request.

Conflicts of Interest: The authors declare no conflicts of interest.

References

1. Hänel, K.H.; Cornelissen, C.; Lüscher, B.; Baron, J.M. Cytokines and the skin barrier. *Int. J. Mol. Sci.* **2013**, *14*, 6720–6745. [CrossRef] [PubMed]
2. Morizane, S.; Mukai, T.; Sunagawa, K.; Tachibana, K.; Kawakami, Y.; Ouchida, M. "Input/output cytokines" in epidermal keratinocytes and the involvement in inflammatory skin diseases. *Front. Immunol.* **2023**, *14*, 1239598. [CrossRef] [PubMed]
3. Liu, B.; Zhu, F.; Xia, X.; Park, E.; Hu, Y. A tale of terminal differentiation: IKKalpha, the master keratinocyte regulator. *Cell Cycle* **2009**, *8*, 527–531. [CrossRef] [PubMed]
4. Lippens, S.; Hoste, E.; Vandenabeele, P.; Agostinis, P.; Declercq, W. Cell death in the skin. *Apoptosis* **2009**, *14*, 549–569. [CrossRef] [PubMed]
5. Zutterman, N.; Maes, H.; Claerhout, S.; Agostinis, P.; Garmyn, M. Deregulation of cell-death pathways as the cornerstone of skin diseases. *Clin. Exp. Dermatol.* **2010**, *35*, 569–575. [CrossRef] [PubMed]
6. Colombo, I.; Sangiovanni, E.; Maggio, R.; Mattozzi, C.; Zava, S.; Corbett, Y.; Fumagalli, M.; Carlino, C.; Corsetto, P.A.; Scaccabarozzi, D.; et al. HaCaT cells as a reliable in vitro differentiation model to dissect the inflammatory/repair response of human keratinocytes. *Mediat. Inflamm.* **2017**, *2017*, 7435621. [CrossRef] [PubMed]
7. Park, K.; Lee, J.H.; Cho, H.C.; Cho, S.Y.; Cho, J.W. Down-regulation of IL-6, IL-8, TNF-α and IL-1β by glucosamine in HaCaT cells, but not in the presence of TNF-α. *Oncol. Lett.* **2010**, *1*, 289–292. [CrossRef] [PubMed]
8. Grimstad, Ø.; Husebye, H.; Espevik, T. TLR3 mediates release of IL-1β and cell death in keratinocytes in a caspase-4 dependent manner. *J. Dermatol. Sci.* **2013**, *72*, 45–53. [CrossRef] [PubMed]
9. Agrawal, R.; Hu, A.; Bollag, W.B. The skin and inflamm-aging. *Biology* **2023**, *12*, 1396. [CrossRef] [PubMed]
10. Hong, M.; Xiao, K.; Lin, P.; Lin, J. Five Rutaceae family ethanol extracts alleviate H_2O_2 and LPS-induced inflammation via NF-κB and JAK-STAT3 pathway in HaCaT cells. *Chin. J. Nat. Med.* **2022**, *20*, 937–947. [CrossRef] [PubMed]
11. Kim, J.; Jung, E.; Yang, W.; Kim, C.K.; Durnaoglu, S.; Oh, I.R.; Kim, C.W.; Sinskey, A.J.; Mihm, M.C., Jr.; Lee, J.H.A. Novel multi-component formulation reduces inflammation in vitro and clinically lessens the symptoms of chronic eczematous skin. *Int. J. Mol. Sci.* **2023**, *24*, 12979. [CrossRef] [PubMed]
12. Anderton, H.; Alqudah, S. Cell death in skin function, inflammation, and disease. *Biochem. J.* **2022**, *479*, 1621–1651. [CrossRef] [PubMed]
13. Neuman, M.G.; Haber, J.A.; Malkiewicz, I.M.; Cameron, R.G.; Katz, G.G.; Shear, N.H. Ethanol signals for apoptosis in cultured skin cells. *Alcohol* **2002**, *26*, 179–190. [CrossRef] [PubMed]
14. He, Y.; Kim, B.G.; Kim, H.E.; Sun, Q.; Shi, S.; Ma, G.; Kim, Y.; Kim, O.S.; Kim, O.J. The protective role of feruloylserotonin in LPS-induced HaCaT cells. *Molecules* **2019**, *24*, 3064. [CrossRef] [PubMed]
15. An, J.Y.; Kim, S.Y.; Kim, H.J.; Bae, H.J.; Lee, H.D.; Choi, Y.Y.; Cho, Y.E.; Cho, S.Y.; Lee, S.J.; Lee, S.; et al. Geraniin from the methanol extract of *Pilea mongolica* suppresses LPS-induced inflammatory responses by inhibiting IRAK4/MAPKs/NF-κB/AP-1 pathway in HaCaT cells. *Int. Immunopharmacol.* **2024**, *140*, 112767. [CrossRef] [PubMed]

16. Wang, M.; Feng, J.; Zhou, D.; Wang, J. Bacterial lipopolysaccharide-induced endothelial activation and dysfunction: A new predictive and therapeutic paradigm for sepsis. *Eur. J. Med. Res.* **2023**, *28*, 339. [CrossRef] [PubMed]
17. Takada, K.; Komine-Aizawa, S.; Hirohata, N.; Trinh, Q.D.; Nishina, A.; Kimura, H.; Hayakawa, S. Poly I:C induces collective migration of HaCaT keratinocytes via IL-8. *BMC Immunol.* **2017**, *18*, 19. [CrossRef] [PubMed]
18. Wan, H.; Yang, H.; Wei, M.; Chen, W. Polyinosinic:polycytidylic acid aggravates calcipotriol-induced atopic dermatitis-like skin lesions in mice by increasing the expression of thymic stromal lymphopoietin. *Ann. Transl. Med.* **2022**, *10*, 209. [CrossRef] [PubMed]
19. Afshari, M.; Kolackova, M.; Rosecka, M.; Čelakovská, J.; Krejsek, J. Unraveling the skin; a comprehensive review of atopic dermatitis, current understanding, and approaches. *Front Immunol.* **2024**, *15*, 1361005. [CrossRef] [PubMed]
20. Zhan, Z.Y.; Jiang, M.; Zhang, Z.H.; An, Y.M.; Wang, X.Y.; Wu, Y.L.; Nan, J.X.; Lian, L.H. NETs contribute to psoriasiform skin inflammation: A novel therapeutic approach targeting IL-36 cytokines by a small molecule tetrahydroxystilbene glucoside. *Phytomedicine* **2024**, *131*, 155783. [CrossRef] [PubMed]
21. Rana, A.A.; Lucs, A.V.; DeVoti, J.; Blanc, L.; Papoin, J.; Wu, R.; Papayannakos, C.J.; Abramson, A.; Bonagura, V.R.; Steinberg, B.M. Poly(I:C) induces controlled release of IL-36γ from keratinocytes in the absence of cell death. *Immunol. Res.* **2015**, *63*, 228–235. [CrossRef] [PubMed]
22. Cetin, M.F.; Hacioglu, C.; Karadeniz, B.; Karadeniz, F.; Tuncer, S. Wound-healing potential of a novel *Helichrysum italicum* film-forming gel: Enhanced bioactivity through sustained delivery and fibroblast modulation. *J. Pharm. Innov.* **2026**, *21*, 307. [CrossRef]
23. Ornano, L.; Venditti, A.; Sanna, C.; Ballero, M.; Maggi, F.; Lupidi, G.; Bramucci, M.; Quassinti, L.; Bianco, A. Chemical composition and biological activity of the essential oil from *Helichrysum microphyllum* Cambess. ssp. *tyrrhenicum* Bacch., Brullo e Giusso growing in La Maddalena Archipelago, Sardinia. *J. Oleo Sci.* **2015**, *64*, 19–26. [CrossRef] [PubMed]
24. Appendino, G.; Ottino, M.; Marquez, N.; Bianchi, F.; Giana, A.; Ballero, M.; Sterner, O.; Fiebich, B.L.; Munoz, E. Arzanol, an anti-inflammatory and anti-HIV-1 phloroglucinol alpha-pyrone from *Helichrysum italicum* ssp. *microphyllum*. *J. Nat. Prod.* **2007**, *70*, 608–612. [CrossRef] [PubMed]
25. Juliano, C.; Marchetti, M.; Campagna, P.; Usai, M. Antimicrobial activity and chemical composition of essential oil from *Helichrysum microphyllum* Cambess. subsp. *tyrrhenicum* Bacch., Brullo & Giusso collected in South-West Sardinia. *Saudi J. Biol. Sci.* **2019**, *26*, 897–905. [CrossRef] [PubMed]
26. Rosa, A.; Atzeri, A.; Nieddu, M.; Appendino, G. New insights into the antioxidant activity and cytotoxicity of arzanol and effect of methylation on its biological properties. *Chem. Phys. Lipids* **2017**, *205*, 55–64. [CrossRef] [PubMed]
27. Deitersen, J.; Berning, L.; Stuhldreier, F.; Ceccacci, S.; Schlütermann, D.; Friedrich, A.; Wu, W.; Sun, Y.; Böhler, P.; Berleth, N.; et al. High-throughput screening for natural compound-based autophagy modulators reveals novel chemotherapeutic mode of action for arzanol. *Cell Death Dis.* **2021**, *12*, 560. [CrossRef] [PubMed]
28. Taglialatela-Scafati, O.; Pollastro, F.; Chianese, G.; Minassi, A.; Gibbons, S.; Arunotayanun, W.; Mabebie, B.; Ballero, M.; Appendino, G. Antimicrobial phenolics and unusual glycerides from *Helichrysum italicum* subsp. *microphyllum*. *J. Nat. Prod.* **2013**, *76*, 346–353. [CrossRef] [PubMed]
29. Rosa, A.; Deiana, M.; Atzeri, A.; Corona, G.; Incani, A.; Melis, M.P.; Appendino, G.; Dessì, M.A. Evaluation of the antioxidant and cytotoxic activity of arzanol, a prenylated alpha-pyrone-phloroglucinol etherodimer from *Helichrysum italicum* subsp. *microphyllum*. *Chem. Biol. Interact.* **2007**, *165*, 117–126. [CrossRef] [PubMed]
30. Rosa, A.; Pollastro, F.; Atzeri, A.; Appendino, G.; Melis, M.P.; Deiana, M.; Incani, A.; Loru, D.; Dessì, M.A. Protective role of arzanol against lipid peroxidation in biological systems. *Chem. Phys. Lipids.* **2011**, *164*, 24–32. [CrossRef] [PubMed]
31. Mammino, L. Intramolecular hydrogen bonding and conformational preferences of arzanol-an antioxidant acylphloroglucinol. *Molecules* **2017**, *22*, 1294. [CrossRef] [PubMed]
32. Piras, F.; Sogos, V.; Pollastro, F.; Appendino, G.; Rosa, A. Arzanol, a natural phloroglucinol α-pyrone, protects HaCaT keratinocytes against H_2O_2-induced oxidative stress, counteracting cytotoxicity, reactive oxygen species generation, apoptosis, and mitochondrial depolarization. *J. Appl. Toxicol.* **2024**, *44*, 720–732. [CrossRef] [PubMed]
33. Piras, F.; Sogos, V.; Pollastro, F.; Rosa, A. Protective Effect of Arzanol against H_2O_2-Induced Oxidative Stress Damage in Differentiated and Undifferentiated SH-SY5Y Cells. *Int. J. Mol. Sci.* **2024**, *25*, 7386. [CrossRef] [PubMed]
34. Bauer, J.; Koeberle, A.; Dehm, F.; Pollastro, F.; Appendino, G.; Northoff, H.; Rossi, A.; Sautebin, L.; Werz, O. Arzanol, a prenylated heterodimeric phloroglucinyl pyrone, inhibits eicosanoid biosynthesis and exhibits anti-inflammatory efficacy in vivo. *Biochem. Pharmakoi.* **2011**, *81*, 259–268. [CrossRef] [PubMed]
35. Kothavade, P.S.; Nagmoti, D.M.; Bulani, V.D.; Juvekar, A.R. Arzanol, a potent mPGES-1 inhibitor: Novel anti-inflammatory agent. *Sci. World J.* **2013**, *2013*, 986429. [CrossRef] [PubMed]
36. Del Gaudio, F.; Pollastro, F.; Mozzicafreddo, M.; Riccio, R.; Minassi, A.; Monti, M.C. Chemoproteomic fishing identifies arzanol as a positive modulator of brain glycogen phosphorylase. *Chem. Commun.* **2018**, *54*, 12863–12866. [CrossRef] [PubMed]

37. Boukamp, P.; Petrussevska, R.T.; Breitkreutz, D.; Hornung, J.; Markham, A.; Fusenig, N.E. Normal keratinization in a spontaneously immortalized aneuploid human keratinocyte cell line. *J. Cell Biol.* **1988**, *106*, 761–771. [CrossRef] [PubMed]
38. Magcwebeba, T.; Riedel, S.; Swanevelder, S.; Bouic, P.; Swart, P.; Gelderblom, W. Interleukin-1α induction in human keratinocytes (HaCaT): An in vitro model for chemoprevention in skin. *J. Skin Cancer.* **2012**, *2012*, 393681. [CrossRef] [PubMed]
39. Park, M.; Woo, S.Y.; Cho, K.A.; Cho, M.S.; Lee, K.H. PD-L1 produced by HaCaT cells under polyinosinic-polycytidylic acid stimulation inhibits melanin production by B16F10 cells. *PLoS ONE* **2020**, *15*, e0233448. [CrossRef] [PubMed]
40. Kok, J.M.L.; Dowd, G.C.; Cabral, J.D.; Wise, L.M. *Macrocystis pyrifera* lipids reduce cytokine-induced pro-inflammatory signalling and barrier dysfunction in human keratinocyte models. *Int. J. Mol. Sci.* **2023**, *24*, 16383. [CrossRef] [PubMed]
41. Mo, X.; Chen, X.; Pan, X.; Lu, Y.; Pan, G.; Xie, J.; Pan, Z.; Li, L.; Tian, H.; Li, Y. Protective effect of *Helianthus annuus* seed byproduct extract on ultraviolet radiation-induced injury in skin cells. *Photochem. Photobiol.* **2024**, *100*, 756–771. [CrossRef] [PubMed]
42. Bao, M.; Hofsink, N.; Plösch, T. LPS versus Poly I:C model: Comparison of long-term effects of bacterial and viral maternal immune activation on the offspring. *Am. J. Physiol. Regul. Integr. Comp. Physiol.* **2022**, *322*, R99–R111. [CrossRef] [PubMed]
43. Liu, X.; Yin, S.; Chen, Y.; Wu, Y.; Zheng, W.; Dong, H.; Bai, Y.; Qin, Y.; Li, J.; Feng, S.; et al. LPS-induced proinflammatory cytokine expression in human airway epithelial cells and macrophages via NF-κB, STAT3 or AP-1 activation. *Mol. Med. Rep.* **2018**, *17*, 5484–5491. [CrossRef] [PubMed]
44. Luo, R.; Yao, Y.; Chen, Z.; Sun, X. An examination of the LPS-TLR4 immune response through the analysis of molecular structures and protein-protein interactions. *Cell Commun. Signal.* **2025**, *23*, 142. [CrossRef] [PubMed]
45. Chen, S.N.; Tan, Y.; Xiao, X.C.; Li, Q.; Wu, Q.; Peng, Y.Y.; Ren, J.; Dong, M.L. Deletion of TLR4 attenuates lipopolysaccharide-induced acute liver injury by inhibiting inflammation and apoptosis. *Acta Pharmacol. Sin.* **2021**, *42*, 1610–1619. [CrossRef] [PubMed]
46. Jeon, S.H.; Lee, M.Y.; Rahman, M.M.; Kim, S.J.; Kim, G.B.; Park, S.Y.; Hong, C.U.; Kim, S.Z.; Kim, J.S.; Kang, H.S. The antioxidant, taurine reduced lipopolysaccharide (LPS)-induced generation of ROS, and activation of MAPKs and Bax in cultured pneumocytes. *Pulm. Pharmacol. Ther.* **2009**, *22*, 562–566. [CrossRef] [PubMed]
47. Wang, S.; Zhang, K.; Song, X.; Huang, Q.; Lin, S.; Deng, S.; Qi, M.; Yang, Y.; Lu, Q.; Zhao, D.; et al. TLR4 Overexpression aggravates bacterial lipopolysaccharide-induced apoptosis via excessive autophagy and NF-κB/MAPK signaling in transgenic mammal models. *Cells* **2023**, *12*, 1769. [CrossRef] [PubMed]
48. Pivarcsi, A.; Bodai, L.; Réthi, B.; Kenderessy-Szabó, A.; Koreck, A.; Széll, M.; Beer, Z.; Bata-Csörgo, Z.; Magócsi, M.; Rajnavölgyi, E.; et al. Expression and function of Toll-like Receptors 2 and 4 in human keratinocytes. *Int. Immunol.* **2003**, *15*, 721–730. [CrossRef] [PubMed]
49. Pivarcsi, A.; Koreck, A.; Bodai, L.; Széll, M.; Szeg, C.; Belso, N.; Kenderessy-Szabó, A.; Bata-Csörgo, Z.; Dobozy, A.; Kemény, L. Differentiation-regulated expression of Toll-like receptors 2 and 4 in HaCaT keratinocytes. *Arch. Dermatol. Res.* **2004**, *296*, 120–124. [CrossRef] [PubMed]
50. Costigan, A.; Hollville, E.; Martin, S.J. Discriminating between apoptosis, necrosis, necroptosis, and ferroptosis by microscopy and flow cytometry. *Curr. Protoc.* **2023**, *3*, e951. [CrossRef] [PubMed]
51. Anany, M.A.; Kreckel, J.; Füllsack, S.; Rosenthal, A.; Otto, C.; Siegmund, D.; Wajant, H. Soluble TNF-like weak inducer of apoptosis (TWEAK) enhances poly(I:C)-induced RIPK1-mediated necroptosis. *Cell Death Dis.* **2018**, *9*, 1084. [CrossRef] [PubMed]
52. Sogos, V.; Caria, P.; Porcedda, C.; Mostallino, R.; Piras, F.; Miliano, C.; De Luca, M.A.; Castelli, M.P. Human neuronal cell lines as an in vitro toxicological tool for the evaluation of novel psychoactive substances. *Int. J. Mol. Sci.* **2021**, *22*, 6785. [CrossRef] [PubMed]
53. Porcedda, C.; Manca, C.; Carta, G.; Piras, F.; Banni, S.; Sogos, V.; Murru, E. Anti-neuroinflammatory effects of conjugated linoleic acid isomers, c9,t11 and t10,c12, on activated BV-2 microglial cells. *Front. Cell. Neurosci.* **2024**, *18*, 1442786. [CrossRef] [PubMed]
54. Zanca, A.; Flegg, J.A.; Osborne, J.M. Push or pull? Cell proliferation and migration during wound healing. *Front. Syst. Biol.* **2022**, *2*, 876075. [CrossRef]
55. Safferling, K.; Sütterlin, T.; Westphal, K.; Ernst, C.; Breuhahn, K.; James, M.; Jäger, D.; Halama, N.; Grabe, N. Wound healing revised: A novel reepithelialization mechanism revealed by in vitro and in silico models. *J. Cell Biol.* **2013**, *4*, 691–709. [CrossRef] [PubMed]
56. Coulombe, P.A. Wound Epithelialization: Accelerating the Pace of Discovery. *J. Investig. Dermatol.* **2003**, *121*, 219–230. [CrossRef] [PubMed]
57. Perrone, P.; D'Angelo, S. Hormesis and health: Molecular mechanisms and the key role of polyphenols. *Food Chem. Adv.* **2025**, *7*, 101030. [CrossRef]
58. Cano Sanchez, M.; Lancel, S.; Boulanger, E.; Neviere, R. Targeting oxidative stress and mitochondrial dysfunction in the treatment of impaired wound healing: A systematic review. *Antioxidants* **2018**, *7*, 98. [CrossRef] [PubMed]